

Stiff-Chain Behavior of Poly(terephthalamide-*p*-benzohydrazide) in Dimethyl Sulfoxide

Kazuo SAKURAI, Kenmei OCHI,* Takashi NORISUYE,
and Hiroshi FUJITA

Department of Macromolecular Science, Osaka University,
Toyonaka, Osaka 560, Japan

(Received April 2, 1984)

ABSTRACT: Fifteen fractionated samples of poly(terephthalamide-*p*-benzohydrazide) (PPAH) ranging in weight-average molecular weight from 2×10^3 to 6×10^4 were studied by light scattering, sedimentation equilibrium, and viscometry with dimethyl sulfoxide (DMSO) at 25°C as the solvent. The data obtained for the radius of gyration, the optical anisotropy factor, and the intrinsic viscosity showed the PPAH chain in DMSO to be semiflexible. Analysis of these data in terms of current theories for the Kratky-Porod wormlike chain gave 11.2 ± 0.5 nm, 185 ± 5 nm⁻¹, 0.5 nm, and 2.1 for the persistence length, molar mass per unit contour length, diameter, and optical anisotropy [$= 3(\alpha_1 - \alpha_2)/(\alpha_1 + 2\alpha_2)$] of the PPAH chain in DMSO, respectively. Here, α_1 and α_2 are, respectively, the longitudinal and transverse polarizabilities per unit contour length of the chain.

KEY WORDS Poly(terephthalamide-*p*-benzohydrazide) / Stiff Chain / Persistence Length / Light Scattering / Radius of Gyration / Optical Anisotropy / Intrinsic Viscosity /

Poly(terephthalamide-*p*-benzohydrazide) (PPAH) is an aromatic polyamide-hydrazide whose repeating unit is shown in Figure 1. It dissolves in dimethyl sulfoxide (DMSO) and *N,N*-dimethylacetamide (DMA).¹

Burke² was the first to find from light scattering and viscosity measurements that the PPAH chain in DMSO is extended. Subsequently, Tsvetkov *et al.*^{3,4} showed that dynamic birefringence, electric birefringence, and viscosity data for PPAH in this solvent are compatible with the Kratky-Porod wormlike chain⁵ with a persistence length q of 27–40 nm. However, light scattering and viscosity measurements on the same system led Bianchi *et al.*^{6,7} to a q value of 3–5 nm, which was smaller by about one order of magnitude than Tsvetkov *et al.*'s. It should be noted that these two groups made data analysis assuming the value of M_L (the molar mass per unit contour

length) to be 188 or 182 nm⁻¹. Hence, their q values have to be accepted with reservation.

In the present study, light scattering, sedimentation equilibrium, and viscosity measurements were made on 15 PPAH fractions in DMSO to determine q and M_L directly. Near completion of the present study, reference was made to a paper of Tsvetkov and Tsepelevich⁸ in which a q of 10–12 nm was deduced from light scattering and viscosity data on 19 unfractionated PPAH samples in DMSO, again assuming M_L to be 200 nm⁻¹. This q is also at variance with the values of other authors^{3,4,6,7} mentioned above.

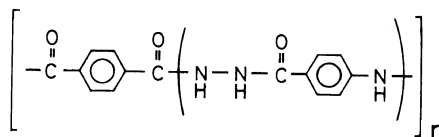


Figure 1. Repeating unit of PPAH.

* Present address: Administration Office, Nishi-Hongwanji Temple, Shimokyo-ku, Kyoto 600, Japan.

EXPERIMENTAL

Samples

Six PPAH samples were prepared by low-temperature solution polycondensation¹ of terephthaloyl chloride and *p*-aminobenzohydrazide in *N*-methyl-2-pyrrolidone or DMA at -8 to 25°C . The yields ranged from 90 to 100%, and the intrinsic viscosities $[\eta]$ (in DMSO at 25°C) from 0.84×10^2 to $6.0 \times 10^2 \text{ cm}^3 \text{ g}^{-1}$. Terephthaloyl chloride was recrystallized twice from hexane; and *p*-aminobenzohydrazide was prepared and purified by the method of Curtius.⁹

Four PPAH samples were chosen from the six prepared, and fractionated by the method described below.

A DMSO–dichloromethane (DCM) mixture (50–70% DCM by volume) was added to a DMSO solution (0.6–0.2% polymer) of a given PPAH sample under stirring at 25°C until the solution became turbid. When the solution was cooled to 0 or -20°C and kept at either temperature for 3–10 h, its turbidity almost disappeared. The clear solution was warmed under stirring until it again became turbid. This occurred at 25°C . After it was allowed to stand for several hours at this temperature, the turbid solution was centrifuged at 1.6×10^4 times gravity for 0.5–3 h. The gel phase was separated and dissolved in DMSO, and the polymer was reprecipitated in water. The supernatant phase was subjected to further fractional precipitation. By repeating such a procedure, each sample was divided into three to seven parts. Fractions having nearly identical $[\eta]$ (in DMSO at 25°C) were combined and further fractionated.

In this way, about 60 fractions were extracted from the four original samples. Fifteen fractions were selected for the present study and designated as f-1, f-2, \dots , f-15. They were reprecipitated from DMSO solutions in water, washed with water more than ten times and then with acetone several times, and finally dried *in vacuo* for about one week at room

temperature.

Light Scattering

Intensities $I_{Uv}(\theta)$ and $I_{Hv}(\theta)$ of light scattered from DMSO solutions of PPAH at 25°C were measured on a Fica 50 light scattering photometer in an angular range from 30 to 150° . Here, $I_{Uv}(\theta)$ denotes the scattering intensity measured at a scattering angle θ with a vertically oriented polarizer and no analyzer, and $I_{Hv}(\theta)$ the scattering intensity measured with a vertically oriented polarizer and a horizontally oriented analyzer. Light of 436 and 546 nm wavelengths was used for all measurements; in each measurement at 436 nm, a 436 nm filter was placed in front of the photomultiplier to minimize fluorescence effects² on $I_{Uv}(\theta)$ and $I_{Hv}(\theta)$. Three PPAH samples f-3, f-5, and f-9 in DMA containing 0.5 wt% acetic acid (DMA–0.5%Ac) were also investigated to check their weight-average molecular weights M_w determined in DMSO.

The apparatus was calibrated with benzene at 25°C as the standard liquid, taking the Rayleigh ratio to be $46.5 \times 10^{-6} \text{ cm}^{-1}$ for 436 nm and $16.1 \times 10^{-6} \text{ cm}^{-1}$ for 546 nm.¹⁰ The depolarization ratio of this liquid was determined to be 0.405 for 436 nm and 0.400 for 546 nm by Rubingh–Yu's method.¹¹

DMSO and DMA–0.5%Ac solutions were made optically clean by 2 h centrifugation at 1.6×10^4 of gravity; DMA–0.5%Ac solutions were filtered through a Millipore's 0.2 μm membrane filter (Type FG) before centrifugation.

Refractive index increments ($\partial n/\partial c$) for PPAH at 436 and 546 nm were, respectively, 0.240 and $0.205 \text{ cm}^3 \text{ g}^{-1}$ in DMSO and 0.288 and $0.248 \text{ cm}^3 \text{ g}^{-1}$ in DMA–0.5%Ac, all at 25°C .

Correction for Absorption

DMSO and DMA–0.5%Ac solutions absorbed 436-nm light. The absorption coefficient γ , determined on a JASCO UVIDEÇ-5A spectrophotometer, ranged from 1–9

cm² g⁻¹ at 436 nm, depending on the polymer sample and solvent, while it was zero at 546 nm. The reduced scattering intensities $R'_{Uv}(\theta)$ derived from $I_{Uv}(\theta)$ for 436 nm were corrected for absorption by the well-known equation¹²

$$R_{Uv}(\theta) = R'_{Uv}(\theta) \exp(2.303\gamma lc) \quad (1)$$

where l is the inner diameter of the light scattering cell (2 cm for our cells) and c , the polymer mass concentration. The values of $R'_{Hv}(\theta)/K$ for 436 and 546 nm agreed so closely that no absorption correction was made for $R'_{Hv}(\theta)$, where K is an optical constant (see eq 3).

Correction for Optical Anisotropy

Figure 2 shows the plots of $(1 + \cos^2 \theta)Kc / 2R_{Uu}(\theta)$ vs. $\sin^2(\theta/2)$ for sample f-9 in DMSO, where $R_{Uu}(\theta)$ is the reduced scattering intensity determined with no polarizer and analyzer used. The data points for each c give a curve having a minimum at 90°, indicating the PPAH chain in DMSO to be optically anisotropic.

According to the current light scattering theory^{13,14} for an optically anisotropic polymer chain, $R_{Uv}(\theta)$ is expressed by

$$\frac{Kc}{R_{Uv}(\theta)} = \frac{1}{M_{w,app}} \left[1 + 2A_{2,app}M_{w,app}c + \dots + \frac{1}{3} \langle S^2 \rangle_{z,app} \left(\frac{4\pi n_0}{\lambda_0} \right)^2 \sin^2 \frac{\theta}{2} + \dots \right] \quad (2)$$

with

$$K = \frac{4\pi^2 n_0^2}{N_A \lambda_0^4} (\partial n / \partial c)^2 \quad (3)$$

$$M_{w,app} = M_w(1 + 7\delta) \quad (4)$$

$$A_{2,app} = A_2 / (1 + 7\delta)^2 \quad (5)$$

$$\langle S^2 \rangle_{z,app} = \langle S^2 \rangle_z^* / (1 + 7\delta) \quad (6)$$

where n_0 is the refractive index of the solvent, λ_0 the wavelength of incident light in vacuum, N_A Avogadro's constant, δ the optical aniso-

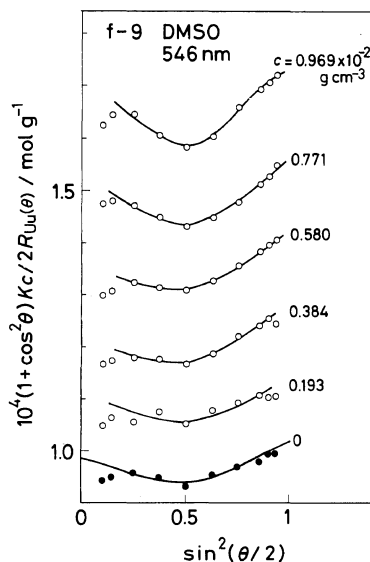


Figure 2. Angular dependence of $(1 + \cos^2 \theta)Kc / 2R_{Uu}(\theta)$ for PPAH sample f-9 in DMSO at 25°C. The curve for $c=0$ represents the theoretical values calculated from Nagai's theory¹⁴ with $q=11.2$ nm, $M_L=185$ nm⁻¹, and $\epsilon=2.1$.

tropy factor, A_2 the second virial coefficient of the solution, and $\langle S^2 \rangle_z^*$ an apparent z -average mean square radius of gyration. It should be noted that except for Gaussian chains, $\langle S^2 \rangle_z^*$ differs from the true z -average mean square radius of gyration $\langle S^2 \rangle_z$ unless δ is zero.¹⁴

In the present study, $R_{Hv}(\theta)$ data were combined either with the $R_{Uv}(\theta)$ data or with the M_w values determined by ultracentrifugation to estimate δ by the general relations¹⁴

$$\lim_{\substack{c \rightarrow 0 \\ \theta \rightarrow 0}} [R_{Hv}(\theta)/Kc] \Big/ \lim_{\substack{c \rightarrow 0 \\ \theta \rightarrow 0}} [R_{Uv}(\theta)/Kc] = 3\delta / (1 + 7\delta) \quad (7)$$

$$\lim_{c \rightarrow 0} [R_{Uv}(\theta)/Kc] = 3\delta M_w \quad (8)$$

With δ so obtained, M_w , A_2 , and $\langle S^2 \rangle_z^*$ for each sample were evaluated from eq 4–6. It should be noted that a suitable model must be assumed for the PPAH chain to estimate $\langle S^2 \rangle_z$ from $\langle S^2 \rangle_z^*$.

Sedimentation Equilibrium

Sedimentation equilibrium measurements were made on PPAH samples f-5, f-8, f-10—f-15 in DMSO in a Beckman Model E ultracentrifuge. A Kel-F 12-mm double-sector cell was used, and the liquid column was adjusted to 1.5–2.0 mm. The rotor speed in rpm was 3×10^4 for samples f-10—f-15, 2.5×10^4 for sample f-8, and 2×10^4 for sample f-5.

The partial specific volume \bar{v} was determined to be $0.676 \text{ cm}^3 \text{ g}^{-1}$.

Viscometry

Intrinsic viscosity of PPAH in DMSO at 25°C was determined using capillary viscometers of the Ubbelohde type. No correction for shear rate effect was necessary for any samples studied.

RESULTS

Figures 3 and 4 illustrate the Zimm plots for sample f-2 in DMSO and sample f-7 in DMA–0.5%Ac, respectively. The values of M_w , A_2 , $\langle S^2 \rangle_z^*$, and δ determined from light scattering measurements are summarized in Table I, along with those of M_w and M_z/M_w (M_z is the z-average molecular weight) from sedimentation equilibrium measurements. Since M_w , $\langle S^2 \rangle_z^*$, and A_2 obtained for 436 and 546 nm agreed within $\pm 1\%$, $\pm 2\%$, and $\pm 4\%$, respectively, their averages have been presented in this table. It can be seen that the M_w values obtained under different experimental conditions agree within $\pm 3\%$.

Apparent characteristic ratios $\langle S^2 \rangle_z^*/M_w$ for PPAH in DMSO are plotted double-logarithmically against M_w in Figure 5, in which the data of Bianchi *et al.*⁶ and Tsvetkov and Tsepelevich⁸ are also shown. Our $\langle S^2 \rangle_z^*/M_w$ increases monotonically with increasing M_w and appears to level off at $2 \times 10^{-2} \text{ nm}^2$. This asymptotic value is comparable with the corresponding value of $\langle S^2 \rangle_z/M_w$ for poly(hexyl isocyanate),¹⁵ a typical semiflexible polymer, in hexane.

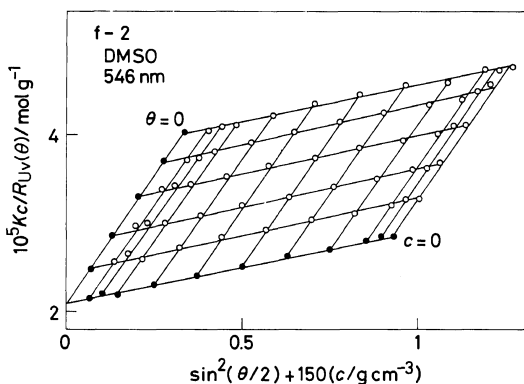


Figure 3. Zimm plot for PPAH sample f-2 in DMSO at 25°C .

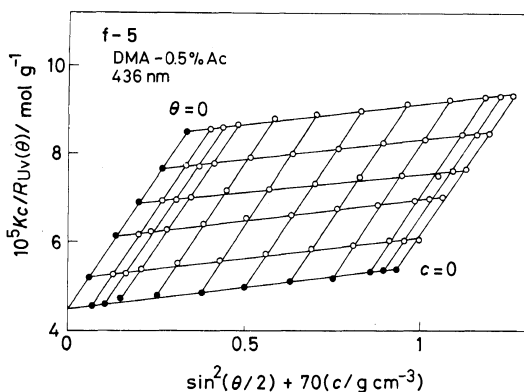


Figure 4. Zimm plot for PPAH sample f-5 in DMA–0.5%Ac at 25°C .

The molecular weight dependence of δ is illustrated in Figure 6. The data points are fitted by a straight line with a slope of -1 for M_w above 1×10^4 and deviate downward from it for lower M_w . This molecular weight dependence of δ is consistent with the theoretical prediction of Nagai¹⁴ for optically anisotropic wormlike chains.

Table II summarizes the values of $[\eta]$ and k' (the Huggins constant) for PPAH samples in DMSO at 25°C . These $[\eta]$ are plotted against M_w in Figure 7, along with the data of Burke,² Bianchi *et al.*,⁷ and Tsvetkov and Tsepelevich.⁸ Our data points are fitted by a smooth curve, whose slope is about 1.3 in the region of M_w below 4×10^3 and decreases continuously to

Polyamide Hydrazide

Table I. Results from light scattering and sedimentation equilibrium measurements on PPAH samples in DMSO at 25°C

Sample	Light scattering					Sedimentation equilibrium		
	$10^{-3}M_w$	10^3A_2	$\langle S^2 \rangle_z^*$	$\langle S^2 \rangle_z$	$10^3\delta$	$10^{-3}M_w$	10^3A_2	M_z
		$\text{cm}^3 \text{mol g}^{-2}$	nm^2	nm^2			$\text{cm}^3 \text{mol g}^{-2}$	M_w
f-1	57.8	3.42	1220	1240	2.6	—	—	—
f-2	48.6	4.82	1110	1130	3.2	—	—	—
f-3	36.6	4.33	728	748	3.8	—	—	—
	37.8 ^a	3.86 ^a	739 ^a	—	2.4 ^a	—	—	—
f-4	28.8	4.82	566	585	4.9	—	—	—
f-5	22.1	4.94	441	459	5.6	22.2	5.40	1.1
	21.5 ^a	4.80 ^a	411 ^a	—	4.7 ^a	—	—	—
f-6	18.2	4.25	334	351	7.8	—	—	—
f-7	15.3	4.86	269	285	8.7	—	—	—
f-8	12.3	5.11	190	205	9.5	12.2	6.47	1.4
f-9	9.35	4.35	130	14 ₃	13	—	—	—
	9.37 ^a	4.84 ^a	12 ₀ ^a	—	9.7 ^a	—	—	—
f-10	6.30	5.78	—	—	17	6.33	6.34	1.2
f-11	—	—	—	—	18	5.68	7.04	1.2
f-12	—	—	—	—	20	4.67	6.45	1.2
f-13	—	—	—	—	30	3.44	7.40	—
f-14	—	—	—	—	35	2.74	7.68	—
f-15	—	—	—	—	—	1.98	7.80	—

^a In DMA-0.5%Ac.

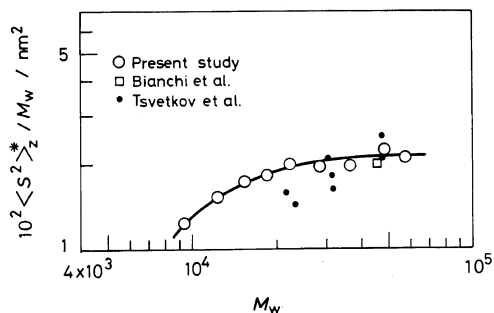


Figure 5. Molecular weight dependence of $\langle S^2 \rangle_z^*/M_w$ for PPAH in DMSO at 25°C.

0.9 with increasing M_w in the higher molecular weight region. This change in slope confirms the conclusion of previous workers^{2-4,6-8} that the PPAH chain in DMSO is semiflexible.

DISCUSSION

Determination of Wormlike Chain Parameters

1. Analysis of $\langle S^2 \rangle_z^*$ Data

Murakami *et al.*¹⁵ showed that Benoit-

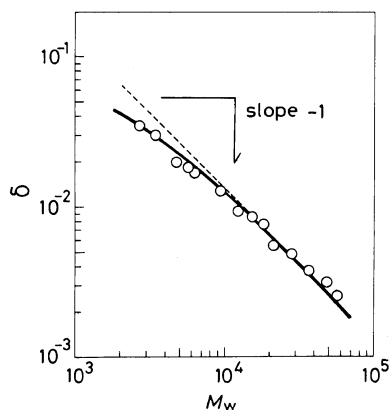


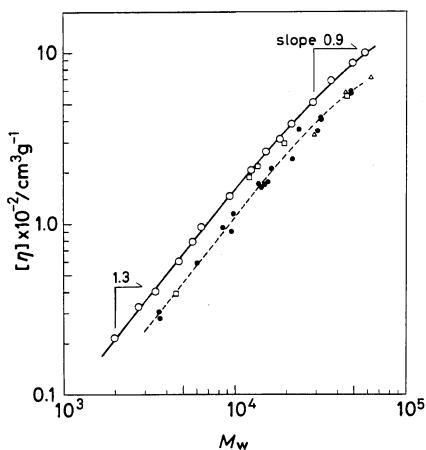
Figure 6. Molecular weight dependence of δ for PPAH in DMSO at 25°C. The solid line represents the theoretical values calculated from eq 15 with $q=11.2 \text{ nm}$, $M_L=185 \text{ nm}^{-1}$, and $\epsilon=2.1$.

Doty's expression¹⁶ for $\langle S^2 \rangle$ of an unperturbed wormlike chain can be approximated by

$$\begin{aligned} & (M/\langle S^2 \rangle)^{1/2} \\ &= (3M_L/q)^{1/2} + 3M_L(3qM_L)^{1/2}/2M \end{aligned} \quad (9)$$

Table II. Results from viscosity measurements on PPAH samples in DMSO at 25°C

Sample	$[\eta] \times 10^{-2}$ cm ³ g ⁻¹	k'
f-1	10.0	0.42
f-2	8.70	0.42
f-3	6.90	0.41
f-4	5.11	0.40
f-5	3.80	0.41
f-6	3.14	0.40
f-7	2.61	0.40
f-8	2.07	0.41
f-9	1.46	0.39
f-10	0.955	0.40
f-11	0.785	0.39
f-12	0.605	0.42
f-13	0.401	0.42
f-14	0.329	0.47
f-15	0.215	0.57

**Figure 7.** Molecular weight dependence of $[\eta]$ for PPAH in DMSO at 25°C. (○), this work; (△), Burke²; (□), Bianchi *et al.*⁷; (●), Tsvetkov and Tsepelevich.⁸

with an error (in $\langle S^2 \rangle$) less than 1%, provided that the Kuhn statistical segment number n_K ($\equiv M/2qM_L$) is larger than 2. For a polydisperse sample, this equation may be replaced by $(M_w/\langle S^2 \rangle_z)^{1/2}$

$$= (3\bar{M}_L/q)^{1/2} + 3\bar{M}_L(3q\bar{M}_L)^{1/2}/2M_w \quad (10)$$

with

$$\bar{M}_L = (M_w/M_z)M_L \quad (11)$$

Thus, q and \bar{M}_L for a polymer may be evaluated from the intercept and slope of a plot of $(M_w/\langle S^2 \rangle_z)^{1/2}$ vs. M_w^{-1} . Further, when the value of M_z/M_w is available for a given sample, M_L can be determined from eq 11. However, this data analysis cannot be made for our $\langle S^2 \rangle_z^*$ data, since as mentioned above, $\langle S^2 \rangle_z^*$ for PPAH should differ from $\langle S^2 \rangle_z$.

Nagai's expression¹⁴ for $\langle S^2 \rangle_z^*$ of an optically anisotropic wormlike chain can be written

$$\langle S^2 \rangle_z^* = \langle S^2 \rangle - f_{UV} \quad (12)$$

with

$$f_{UV} = \frac{4q^2}{45} \left[\varepsilon \left(1 - \frac{8qM_L}{3M} + \frac{26q^2M_L^2}{9M^2} \right) - \frac{\varepsilon^2}{126} \left(\frac{23qM_L}{M} - \frac{103q^2M_L^2}{3M^2} \right) \right] \quad (13)$$

and

$$\varepsilon = 3(\alpha_1 - \alpha_2)/(\alpha_1 + 2\alpha_2) \quad (14)$$

provided $n_K > 2$. Here, α_1 and α_2 are, respectively, the longitudinal and transverse polarizabilities per unit contour length of the chain, and ε is related to δ by¹⁴

$$\delta = \frac{2\varepsilon^2 q M_L}{135M} \left[1 - \frac{qM_L}{3M} (1 - e^{-3M/qM_L}) \right] \quad (15)$$

Since f_{UV} is a function of q , M_L , and ε , these three parameters must be estimated to evaluate $\langle S^2 \rangle_z$ from $\langle S^2 \rangle_z^*$. Hence, all equations 10–15 must be combined in order to determine q and M_L of PPAH in DMSO.

In the present study, the values of q , M_L , ε , and $\langle S^2 \rangle_z$ were determined by the following iteration method.

Step 1. Approximate values of q and \bar{M}_L were estimated from the intercept and slope of a $(M_w/\langle S^2 \rangle_z^*)^{1/2}$ vs. M_w^{-1} plot. With \bar{M}_L so obtained and an M_z/M_w value of 1.22 (the average of the M_z/M_w values in Table I), M_L was evaluated from eq 11.

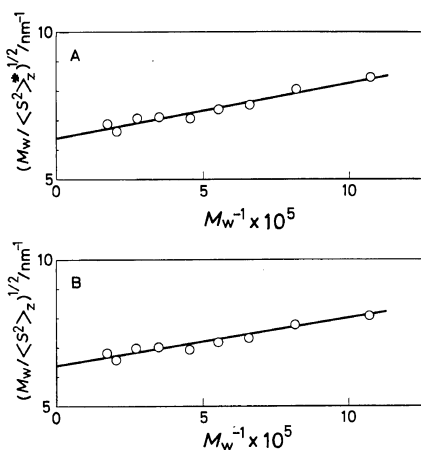


Figure 8. Plots of $(M_w / \langle S^2 \rangle_z)^{1/2}$ and $(M_w / \langle S^2 \rangle_z)^{1/2}$ vs. M_w^{-1} for PPAH in DMSO.

Step 2. These first approximations to q and M_L were used to find ε which led eq 15 to a close agreement with our experimental δ ; ε for PPAH in DMSO is known to be positive.³

Step 3. The correction term f_{Uv} was calculated using the q , M_L , and ε obtained, and $\langle S^2 \rangle_z$ for the samples were evaluated.

Step 4. With these $\langle S^2 \rangle_z$ values, a plot of $(M_w / \langle S^2 \rangle_z)^{1/2}$ vs. M_w^{-1} was reconstructed and used to iterate steps 1–3. This process was repeated until convergent values of q , M_L , ε , and $\langle S^2 \rangle_z$ were reached.

Actually, the following convergent values were obtained after iteration was done twice: $q = 11.2 \pm 0.5$ nm, $M_L = 185 \pm 5$ nm⁻¹, and $\varepsilon = 2.1$. Figures 8A and 8B show the plots of $(M_w / \langle S^2 \rangle_z)^{1/2}$ vs. M_w^{-1} (the first step) and $(M_w / \langle S^2 \rangle_z)^{1/2}$ vs. M_w^{-1} (the final step), respectively. The $\langle S^2 \rangle_z$ values obtained appear in the fifth column of Table I. The M_L value of 185 nm⁻¹ is very close to 190 nm⁻¹ estimated from crystallographic data^{17,18} for PPAH and also to 180–190 nm⁻¹ determined by Krigbaum and Sasaki¹⁹ who used small-angle X-ray scattering data in DMA-0.5%Ac.

In Figures 9 and 6, respectively, our $\langle S^2 \rangle_z$ and δ data are compared with the theoretical values (the solid lines) computed from Benoit-Doty's expression¹⁶ and eq 15 with $q =$

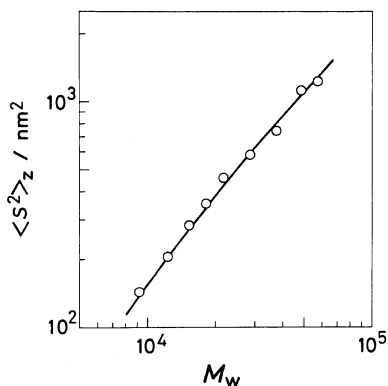


Figure 9. Comparison of $\langle S^2 \rangle_z$ for PPAH in DMSO with the theoretical values (the solid line) calculated from Benoit-Doty's expression¹⁶ with $q = 11.2$ nm and $M_L = 152$ nm⁻¹ ($M_L = 185$ nm⁻¹, $M_z/M_w = 1.22$).

11.2 nm, $M_L = 185$ nm⁻¹, and $\varepsilon = 2.1$. The agreement between theory and experiment in both graphs substantiates that the statistical properties of the PPAH chain in DMSO can be described accurately by an unperturbed wormlike chain with these parameter values.

The solid line for $c = 0$ in Figure 2 has been calculated from Nagai's theory¹⁴ for optically anisotropic wormlike chains using the same set of q , M_L , and ε as above. It can be seen that the Nagai theory describes the observed angular dependence of $[(1 + \cos^2 \theta)Kc/2R_{Uv}(\theta)]_{c=0}$.

2. Analysis of $[\eta]$ Data

Bushin *et al.*²⁰ and Bohdanecký²¹ independently showed that Yamakawa-Fujii-Yoshizaki's theory^{22,23} for $[\eta]$ of an unperturbed wormlike cylinder can be replaced approximately by

$$(M^2/[\eta])^{1/3} = A + BM^{1/2} \quad (16)$$

with

$$A = 1.516 \times 10^{-8} A_0 M_L \quad (\text{g}^{1/3} \text{cm}^{-1}) \quad (17)$$

$$B = 1.516 \times 10^{-8} B_0 (2q/M_L)^{-1/2} \quad (\text{g}^{1/3} \text{cm}^{-1}) \quad (18)$$

where A_0 and B_0 are known functions of $d/2q$ (d is the diameter of the cylinder). The function

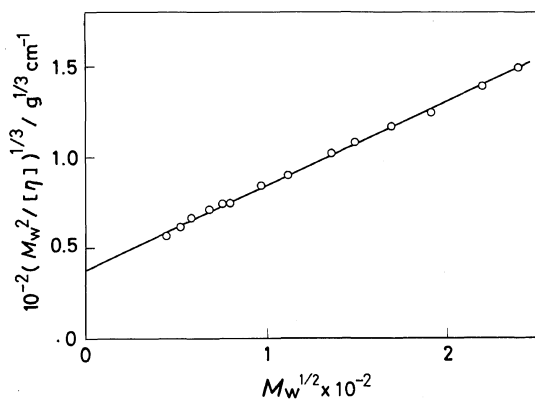


Figure 10. Plot of $(M_w^2/[\eta])^{1/3}$ vs. $M_w^{1/2}$ for PPAH in DMSO.

B_0 is so insensitive to $d/2q$ that it may be equated to 1.05 for $d/2q$ ranging from 0.005 to 0.08.²¹

Figure 10 shows the plot of $(M_w^2/[\eta])^{1/3}$ vs. $M_w^{1/2}$ constructed from our $[\eta]$ data. As predicted by eq 16, the data points can be fitted by a straight line which gives $38.0 \text{ g}^{1/3} \text{ cm}^{-1}$ and $0.463 \text{ g}^{1/3} \text{ cm}^{-1}$ for A and B , respectively. This B value is close to $0.457 \text{ g}^{1/3} \text{ cm}^{-1}$ estimated from eq 18 with $B_0=1.05$ and the wormlike chain parameters ($q=11.2 \text{ nm}$ and $M_L=185 \text{ nm}^{-1}$) determined above from $\langle S^2 \rangle_z^*$ data. Substitution of $A=38.0 \text{ g}^{1/3} \text{ cm}^{-1}$ and $M_L=185 \text{ nm}^{-1}$ into eq 17 gives 1.35 for A_0 , which in turn yields 2.15×10^{-2} for $d/2q$. With this $d/2q$ value and $q=11.2 \text{ nm}$, the diameter of the PPAH chain in DMSO is determined to be 0.48 nm.

Bohdanecký²¹ proposed a method for determining M_L , q , and d from $[\eta]$ and \bar{v} data by postulating that the hydrodynamic volume occupied by one gram of a wormlike cylinder is equal to \bar{v} . His method applied to our data yielded $q=11.2 \text{ nm}$, $M_L=190 \text{ nm}^{-1}$, and $d=0.5 \text{ nm}$. These values are very close to those determined above from $\langle S^2 \rangle_z^*$ and $[\eta]$ data, indicating Bohdanecký's assumption for \bar{v} to be reasonable for PPAH in DMSO.

Figure 11 compares our $[\eta]$ data for PPAH in DMSO with the theoretical curve com-

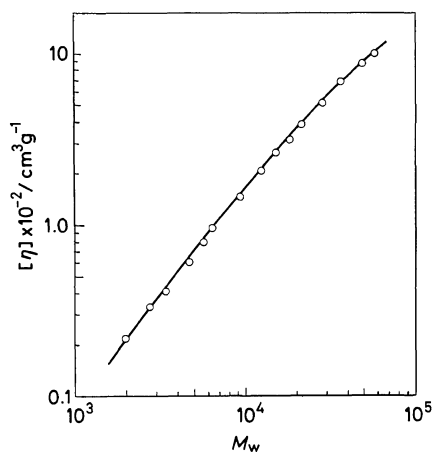


Figure 11. Comparison of measured $[\eta]$ for PPAH in DMSO with theoretical values (the solid line) calculated from Yamakawa–Fujii–Yoshizaki's theory^{22,23} with $q=11.2 \text{ nm}$, $M_L=185 \text{ nm}^{-1}$, and $d=0.5 \text{ nm}$.

Table III. Wormlike chain parameters for PPAH in DMSO

q	M_L	d	Ref
nm	nm^{-1}	nm	
11.2 ± 0.5	185 ± 5	0.5	This work
27–40	(188) ^a	—	Tsvetkov <i>et al.</i> ^{3,4}
3–5	(182) ^a	(0.7) ^a	Bianchi <i>et al.</i> ^{6,7}
10–12	(200) ^a	0.5	Tsvetkov and Tsepelevich ⁸

^a Assumed.

puted from the Yamakawa–Fujii–Yoshizaki theory^{22,23} with $q=11.2 \text{ nm}$, $M_L=185 \text{ nm}^{-1}$, and $d=0.5 \text{ nm}$. The fit of the curve to the data points appears almost perfect.

Comparison with Reported Values of q

Table III compares the q , M_L , and d values from the present work with those determined or assumed by other authors.^{3,4,6–8} Our q essentially confirms that of Tsvetkov and Tsepelevich.⁸ We should like to comment on the q values of Tsvetkov *et al.*^{3,4} and Bianchi *et al.*^{6,7} which appreciably differ from ours.

Tsvetkov *et al.* evaluated the molecular weights of their PPAH samples from $[\eta]$ and

dynamic birefringence data on the basis of a theoretical expression for the characteristic orientation angle for rodlike polymers. Recently, Tsvetkov and Tsepelevich⁸ carried out light scattering measurements on some of these samples and obtained M_w differing considerably from their previous values. Hence, it is required that the dynamic birefringence and electric birefringence data of Tsvetkov *et al.* be reanalyzed in terms of these light scattering M_w so as to estimate a correct q value.

Bianchi *et al.* corrected their $\langle S^2 \rangle_z^*$ and $[\eta]$ data for excluded volume effect, using the Stockmayer-Fixman plot²⁴ applicable only to flexible polymers. This correction led to a q value of 3–5 nm, which is about one-half that estimated from uncorrected $[\eta]$ data.⁷ We have shown above that the PPAH chain in DMSO is unperturbed by volume effects in the entire M_w range studied, which includes all samples studied by Bianchi *et al.* Thus, it must be considered that these authors obtained too small a q value as a result of making unnecessary corrections of their data for this effect.

Acknowledgment. We express our appreciation to Mitsui Toatsu Co. for providing the terephthaloyl chloride.

REFERENCES

1. B. M. Culbertson and R. Murphy, *Polym. Lett.*, **5**, 807 (1967).
2. J. J. Burke, *J. Macromol. Sci.-Chem.*, **A**, **7**, 187 (1973).
3. V. N. Tsvetkov, G. J. Kudriavtsev, N. A. Mikhailova, A. V. Volokhina, and V. D. Kalmykova, *Eur. Polym. J.*, **14**, 475 (1978).
4. V. N. Tsvetkov, I. P. Kolomiets, and A. V. Lezov, *Eur. Polym. J.*, **18**, 373 (1982).
5. O. Kratky and G. Porod, *Rec. Trav. Chim.*, **68**, 1106 (1949).
6. E. Bianchi, A. Ciferri, A. Teadldi, and W. R. Krigbaum, *J. Polym. Sci., Polym. Phys. Ed.*, **17**, 2091 (1979).
7. E. Bianchi, A. Ciferri, J. Preston, and W. R. Krigbaum, *J. Polym. Sci., Polym. Phys. Ed.*, **19**, 863 (1981).
8. V. N. Tsvetkov and S. O. Tsepelevich, *Eur. Polym. J.*, **19**, 267 (1983).
9. T. Curtius, *J. Prakt. Chem.*, **95**, 355 (1917).
10. Gj. Deželić and J. Vavra, *Croat. Chem. Acta*, **38**, 35 (1966).
11. D. N. Rubingh and H. Yu, *Macromolecules*, **9**, 681 (1976).
12. J. L. Lauer, *J. Opt. Soc. Am.*, **41**, 482 (1951).
13. H. Yamakawa, "Modern Theory of Polymer Solutions," Harper and Row, New York, N. Y., 1971, Chapter V.
14. K. Nagai, *Polym. J.*, **3**, 67 (1972).
15. H. Murakami, T. Norisuye, and H. Fujita, *Macromolecules*, **13**, 345 (1980).
16. H. Benoit and P. Doty, *J. Phys. Chem.*, **57**, 958 (1953).
17. V. F. Holland, *J. Macromol. Sci.-Chem.*, **A**, **7**, 173 (1973).
18. R. L. Miller, *J. Macromol. Sci.-Chem.*, **A**, **7**, 183 (1973).
19. W. R. Krigbaum and S. Sasaki, *J. Polym. Sci., Polym. Phys. Ed.*, **19**, 1339 (1981).
20. S. V. Bushin, V. N. Tsvetkov, E. B. Lysenko, and V. N. Emelyanov, *Vysokomol. Soedin., Ser. A*, **23**, 2494 (1981).
21. M. Bohdanecký, *Macromolecules*, **16**, 1483 (1983).
22. H. Yamakawa and M. Fujii, *Macromolecules*, **7**, 128 (1974).
23. H. Yamakawa and T. Yoshizaki, *Macromolecules*, **13**, 633 (1980).
24. W. H. Stockmayer and M. Fixman, *J. Polym. Sci., C*, **1**, 137 (1963).